Optical and radio signatures of negative gigantic jets: Cases from Typhoon Lionrock (2010)

Sung-Ming Huang,[1] Rue-Rou Hsu,[1] Li-Jou Lee,[1] Han-Tzong Su,[1] Cheng-Ling Kuo,[1] Chun-Chieh Wu,[2] Jung-Kuang Chou,[1] Shu-Chun Chang,[1] Yen-Jung Wu,[1] and Alfred B. Chen[3]

Received 7 February 2012; revised 19 June 2012; accepted 20 June 2012; published 4 August 2012.

[1] On 31 August 2010, more than 100 transient luminous events were observed to occur over Typhoon Lionrock when it passed at ~210 km to the southwest of the NCKU site in Taiwan. Among them, 14 negative gigantic jets (GJs) with clear recognizable morphologies and radio frequency signals are analyzed. These GJs are all found to have negative discharge polarity and thus are type I GJs. Morphologically, they are grouped into three forms: tree-like, carrot-like, and a new intermediate type called tree-carrot-like GJs. The ULF and ELF/VLF band signals of these events contain clear signatures associated with GJ development stages, including the initiating lightning, the leading jet, the fully developed jet, and the trailing jet. Though the radio waveform for each group of GJs always contains a fast descending pulse linked with the surge current upon the GJ-ionosphere contact, the detailed waveforms actually vary substantially. Cross analysis of the optical and radio frequency signals for these GJs indicates that a large surge current moment (CM) (>60 kA-km) appears to be essentially associated with the tree-like GJs. In contrast, the carrot-like and the tree-carrot-like GJs are both related to a surge CM less than 36 kA-km, and a continuing CM less than 27 kA-km further separates the carrot-like GJs from the tree-carrot-like GJs. Furthermore, on the peak CM versus charge moment change diagram for the initiating lightning, different groups of GJs seem to exhibit different trends. This feature suggests that the eventual forms of negative GJs may have been determined at the initiating lightning stage.

Citation: Huang, S.-M., R.-R. Hsu, L.-J. Lee, H.-T. Su, C.-L. Kuo, C.-C. Wu, J.-K. Chou, S.-C. Chang, Y.-J. Wu, and A. B. Chen (2012), Optical and radio signatures of negative gigantic jets: Cases from Typhoon Lionrock (2010), *J. Geophys. Res.*, *117*, A08307, doi:10.1029/2012JA017600.

1. Introduction

[2] The gigantic jet (GJ) is a member of the transient luminous event (TLE) [*Pasko*, 2008, 2010; *Pasko et al.*, 2012] family that was first observed by *Pasko et al.* [2002] near Puerto Rico to propagate out from a thundercloud to an altitude of ~70 km. In the following year, *Su et al.* [2003] observed five GJs near Philippines that directly linked the thundercloud top at ~16 km and the ionospheric E layer at ~90 km. From the recorded optical images, *Su et al.* [2003] noted that the evolution of these GJs can be divided into three stages: the leading jet, the fully developed jet (FDJ), and the trailing jet, but whether there were cloud flashes before these events was not clear since the lower field of view (FOV) was blocked by a roof in the foreground. They also reported that there are two morphological forms (the tree-like and the carrot-like) for the fully developed jets [*Su et al.*, 2003]. Furthermore, the associated extremely low frequency (ELF) magnetic field signals of these GJs indicate that they are all negative cloud-to-ionosphere (-CI) events, that transfer negative charge from cloud to ionosphere and have inferred charge moment changes (CMCs) of 1000 to 2000 C-km. Subsequent observations of GJs further indicated that these large-scale CI discharges are a global phenomenon, as deduced from ground campaigns carried out in the Americas [*Pasko et al.*, 2002; *van der Velde et al.*, 2007; *Cummer et al.*, 2009; *Lu et al.*, 2011], Europe [*van der Velde et al.*, 2010], Indian Ocean [*Soula et al.*, 2011], Asia [*Su et al.*, 2003; *Chou et al.*, 2011], and surveys from space [*Chen et al.*, 2008; *Kuo et al.*, 2009; *Chou et al.*, 2010; *Lee et al.*, 2012].

[3] Gigantic jets, blue jets and blue starters belong to a general class of upward discharging TLEs from the

[1]Department of Physics, National Cheng Kung University, Tainan, Taiwan.
[2]Department of Atmospheric Sciences, National Taiwan University, Taipei, Taiwan.
[3]Institute of Space, Astrophysical and Plasma Sciences, National Cheng Kung University, Tainan, Taiwan.

Corresponding authors: A. B. Chen, Institute of Space, Astrophysical and Plasma Sciences, National Cheng Kung University, Tainan 70101, Taiwan. (alfred@phys.ncku.edu.tw)
H.-T. Su, Department of Physics, National Cheng Kung University, Tainan 70101, Taiwan. (htsu@phys.ncku.edu.tw)

0148-0227/12/2012JA017600

thundercloud tops [*Pasko*, 2008, 2010; *Pasko et al.*, 2012]. The most notable feature that separates these jets is the termination height, with the average terminal altitude of about 20.8 km for the blue starters [*Wescott et al.*, 1996], 40–50 km for the blue jets [*Wescott et al.*, 1995; *Boeck et al.*, 1995; *Lyons et al.*, 2003; *Chou et al.*, 2011], and near the local lower ionosphere boundary for the gigantic jets. To elucidate the most favorable conditions leading to the occurrence of GJs, *Krehbiel et al.* [2008] proposed that a negative GJ is mostly likely associated with a charge imbalance between the central negative and upper positive charge layers of a normally electrified thunderstorm; an upward discharge (the GJ initiation) emanates from the middle-level negative charge reservoir and penetrates the cloud top to develop into a GJ. Recent observations also suggest that this charge imbalance might be amplified by the intracloud lightning progression prior to the GJ initiation [*Lu et al.*, 2011]. By studying the luminous evolution of a negative GJ and its associated ultralow frequency (ULF) signal, *Cummer et al.* [2009] reported that a signal associated with the GJ initiation was identified and the inferred CMC for this event is ~10800 C-km in the first second; they also noted that there is a high correlation between the current moment and the brightness of GJ. From detailed analysis of the GJs recorded by the ISUAL experiment [*Chern et al.*, 2003; *Chen et al.*, 2008; *Lee et al.*, 2012], *Kuo et al.* [2009] reported that, after the GJ reaches ionosphere, the ionized gas in the upper truck could short-out the upper discharge channel and cause the local ionosphere boundary to drop down to ~50 km [*Marshall and Inan*, 2007; *Lee et al.*, 2012]; then a current continuously flows between the cloud top and the lower ionosphere. As the boundary recovers its altitude, the contact point moves up and the continuing current manifests itself as a seemingly upward surging trailing jet. Also by studying the ISUAL data, *Chou et al.* [2010] reported there are two discharge types of GJs, with the type I GJ being a negative CI event and the type II GJ being a positive CI discharge. Recently, *Lu et al.* [2011] analyzed the characteristics and the charge evolution of two negative CI GJs that occurred near a very high frequency (VHF) lightning mapping network, and reported the detection of the charge migration from a leader process above the 20 km altitude. The VHF data also indicate that the upward propagation speed of the initiating discharge is similar to that of the leading jet reported in *Su et al.* [2003].

[4] In short, the current state of the knowledge on the negative GJ is: this type of GJs starts with normal intracloud lightning that might exaggerate the charge imbalance in the cloud [*Krehbiel et al.*, 2008; *Lu et al.*, 2011]. A short moment later, another intracloud initiating lightning (the GJ initiation) develops from the midlevel charge reservoir of the cloud and penetrates the cloud top to become a leading jet which will propagate further to reach the ionosphere and to become a GJ. After the upward discharge reaches the ionosphere at the FDJ stage (the GJ-ionosphere contact), the local ionospheric boundary drops and a continuing current flows between the cloud and the lowered local ionosphere. Then, as the local ionosphere regains its original altitude, the continuing current appears as an up-surging trailing jet [*Kuo et al.*, 2009].

[5] In this work, 14 negative GJs and their associated ULF and extremely low frequency/very low frequency (ELF/VLF) band signals are analyzed. From the optical data, two previous reported forms (tree-like and carrot-like) as well as a new intermediate form, termed as "tree-carrot-like GJs" are identified. The association of the ULF and ELF/VLF band signals with the various optical stages of the GJs is presented. The discharging parameters of the GJs are inferred from the radio frequency data, and their possible associations with the observed optical features of these three forms of GJs are discussed. In addition, the meteorological features that caused the Lionrock (2010) to become such a prolific GJ producing system are also elaborated.

2. Instruments

[6] The National Cheng Kung University (NCKU; the black square in Figure 1; latitude: 23.00°N and longitude: 120.22°E) is located at the Tainan City, Taiwan. Since 2001, the NCKU group has been carrying out routine summer optical TLE campaigns from the roof of the Physics Departmental building right in the center of Tainan city [*Su et al.*, 2002; *Hsu et al.*, 2003]. The NCKU optical TLE imaging system consists of two cameras mounted on a remote controllable platform, which is equipped with a digital spirit level and compass; hence the elevation and azimuth angles of the recorded events can be accurately determined. Each camera has a WATEC NEPTUNE 100 CCD equipped with a 12 mm/f1.2 lens (FOV: 30.8° × 23.1°). One camera contains no filter and is thus labeled as the "C camera," while the other camera (the R camera) is fitted with a red-pass filter (passing band: 570 ~ 2700 nm). The WATEC NEPTUNE 100 CCD is sensitive between 320 and 1030 nm, hence the C and the R cameras have effective passing bands of 320 ~ 1030 nm and 570 ~ 1030 nm, respectively. The image frames from the CCDs were further passed through GPS-synchronized time code inserters to imprint the millisecond precision time codes on the video frames. The video footages were stored in the computer hard disc and on digital video tapes at the standard NTSC frame rate (30 frames/second or 60 image fields/second; one field is 16.67 ms). However, the C camera had functioned erratically on the night when the negative GJs reported in this work were recorded. Thus only the video frames from the R camera are analyzed in this work.

[7] The NCKU group also operates two magnetic recording stations. The magnetic ULF station is located at the Lulin Observatory, Yushan National Park in Taiwan (the black cross mark in Figure 1; 23.47°N and 120.87°E) [see *Wang et al.*, 2005; *Huang et al.*, 2011]. The system is based on a pair of EMI-BF4 horizontal magnetic coils which are sensitive in the radio frequency band between 0.3 Hz and 500 Hz, with coils either orientated parallel (H; north south) or perpendicular to (D; east west) the geomagnetic field. The recording system is equipped with a GPS clock and all the data were sampled continuously at 5 kHz. The NCKU ELF/VLF station is located at the Cingcao elementary school which resides in the suburban area of the Tainan City (the black triangle mark in Figure 1; 23.08°N and120.12°E). The system is based on a pair of QUASAR horizontal induction sensors and one vertical electric field sensor, which are sensitive in the radio frequency band of 1.5 Hz to 15 kHz and 0.1 Hz to 100 kHz, respectively. The signals from this system

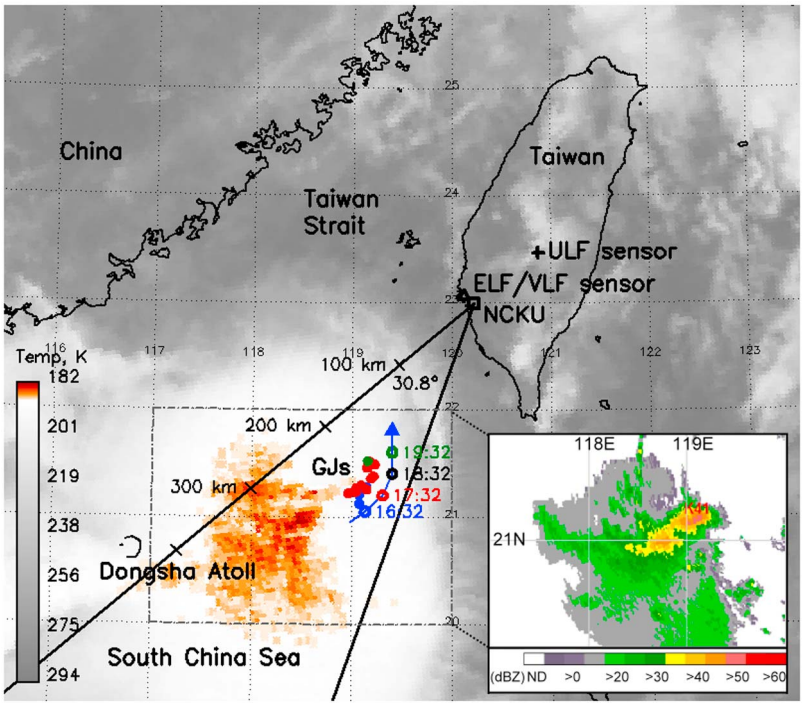

Figure 1. MTSAT-2 infrared map for the surrounding region of Taiwan at 17:32 UTC on 31 August 2010. Typhoon Lionrock can be identified as the big patch of clouds toward the southwest of Taiwan. Inset is the cropped radar reflectivity for the GJ occurring region from the Kenting radar station (21.89°N and 120.85°E; effective range ∼250 km) at 17:30 UTC by Central Weather Bureau (CWB). Overlapping markers on the map, respectively: black square, the optical observation site at NCKU, Tainan City; black triangle, NCKU ELF/VLF station; and black cross, NCKU ULF station. The two black lines extending from the NCKU campus represents the FOV (30.8°) of the cameras. The color circles indicate the storm centers during the observation period between 15:45 and 20:01 UTC (23:45 and 04:01 in local time), with the times listed to the right. The color dots denote the inferred locations of the 14 observed GJs that occurred within a 1 hour bin centering on the times of the storm center.

have been sampled continuously at 100 kHz since August 2010. Owing to a better signal-to-noise ratio (SNR) of the electric field data than the magnetic field data, the analysis of ELF/VLF signal in this work is based on the electric field measurement. The two radio frequency data are used to infer the current moment (CM) and the time-integrated charge moment change (CMC) of the discharge events as functions of time [*Cummer et al.*, 2009].

3. Typhoon Lionrock and the Occurrence of GJs

[8] Typhoon Lionrock (2010) was the first of five typhoons with warning issued by the Central Weather Bureau (CWB) in Taiwan and was named in number as '1006'. It formed as a tropical depression in the vicinity of Dongsha Atoll (20.70°N and 116.73°E) over the northern South China Sea on 27 August and dissipated in southeastern China on 3 September. At the beginning, Lionrock moved northward and intensified into a weak typhoon. Later, the movement of Lionrock was slowed down due to the presence of Typhoon Namtheun (numbered as '1008'), which formed rapidly in northern Taiwan. On 30 August, the Fujiwhara effect (binary interaction [*Wu et al.*, 2003]) between the two typhoons drifted Lionrock eastward and east-southeastward. As Lionrock continued to intensify, it reached the lowest mean sea level pressure of about 985 hPa around 12:00 UTC on 30 August. On 31 August, by combining (merging) the circulation and rainband associated with Namtheun, Lionrock further intensified. Lionrock then changed its course to the north-northeast and reached the maximum sustained winds of 23 ms^{-1}. Between 15:00 and 20:00 UTC, the balloon sounding in the synoptic environment of Lionrock inferred relatively high convective available potential energy (CAPE) of 1980 J/kg and relatively low convective inhibition (CIN) of 70 m^2s^2, thus providing favorable thermodynamic conditions to support vigorous convection in the inner core eyewall region of Typhoon Lionrock with strong dynamic forcing (i.e., convergence in the boundary layer under the eyewall). When Lionrock approached the southern tip of Taiwan, the radar reflectivity measured from Taiwan was around 50 ∼ 60 dBz and the cloud top temperature was around 190 K (−83°C), as estimated from the infrared satellite image. Eventually, Lionrock crossed Taiwan Strait northwestward and made landfall in southeastern China on 2 September. Lionrock then weakened into a tropical storm quickly and dissipated in the next day.

[9] Between 15:45 and 20:01 UTC (23:45 and 04:01 LST) on 31 August 2010, when the center of Typhoon Lionrock was located at about 270 km to 170 km toward the southwest of Taiwan, more than 100 TLEs (including sprites and dozens of gigantic jets) occurred over the typhoon as observed from the NCKU site. Among the identifiable gigantic jets, their locations appear to move synchronously with the typhoon center (Figure 1). However, in the FOV of the cameras, the front edge of the typhoon clouds blocked the lower half of the view and the severe light pollution from Tainan city also affected the observation in classifying some of the events. Therefore, only 14 negative gigantic jets (GJs) that have clear recognizable forms and identifiable ULF/ELF/VLF data are chosen for detailed analysis.

[10] Based on the height inferred from the IRI-2007 model [*Bilitza and Reinisch*, 2008] and the boundaries previously reported in *Su et al.* [2003], *Cummer et al.* [2009], and *Soula et al.* [2011], the nighttime ionospheric boundary for the region above Lionrock is estimated to be located at 90 km in altitude during the occurring window of the observed GJs. The fully developed jets (FDJs) of the GJs is thus assumed to terminate at this ionosphere height, therefore the occurrence locations of the GJs are inferred to be at the positions marked by the color dots in Figure 1. From the radar reflectivity of the Kenting radar station (21.89°N and 120.85°E; effective range ~250 km) at 17:30 UTC, two regions in Lionrock in the GJ occurring region show notable echoes (Figure 1, inset). The strong echo region closer to the NCKU site is a convective cell at the eyewall with cloud top temperature of about 200 K, which corresponds to cloud top height of about 14.5 km. Similar strong echo regions from the deep convective cores also exist in radar reflectivity data obtained at the occurring times of other GJs. Interestingly, the inferred locations of the GJs all collocate with the region with strong radar echo that associated with the eyewall convective core of Lionrock, indicating the observed negative GJs are likely originated from the protruding cloud top region. The soundings also indicate that the direction of the wind rotates clockwise with height, with westerly wind in the lower level and easterly wind at the cloud top at the location of the GJ producing convective core (Figure 1). It is possible that the vertical wind shear may have dislocated the charge structure in the convective core and makes the GJs to occur more easily [*Riousset et al.*, 2010]. Consequently, Lionrock serves as a prolific system in the production of gigantic jets.

[11] To check the fairness of the inferred GJ locations, the worldwide lightning location network (WWLLN) [*Dowden et al.*, 2002] data are also used. One GJ initiating lightning is also found to be a WWLLN event, and the geolocation offset of this WWLLN lightning is found to be 15 km with respect to that of the FDJ-inferred location, thus indicating that the inferred locations of the observed GJs are of reasonable accuracy. However, it should be noted that WWLLN [*Rodger et al.*, 2006] did not actually detect these GJ events. The locating of initiating lightning by no means represents the occurrence location of GJ is known as well, since the location offset between initiating lightning and the GJ is not known. However, if we assume GJ and its initiating lightning have no occurring location offset, from the top elevation angle of the FDJ and the location of the WWLLN detected initiating lightning, the GJ termination height is inferred to be ~95 km [*Hsu et al.*, 2003]. Since these 14 GJs evidently occurred over a relatively small area and their top elevation angles are all similar to the one having WWLLN detected initiating lightning, a 90 km termination height for these GJs would be scientifically sound.

4. The Optical Features of the Negative Gigantic Jets

[12] In this section, the optical band data, flashes associated with the initiating lightning, the morphology, and the luminous duration of GJs are presented.

4.1. The Initiating Lightning of Gigantic Jets

[13] For the 14 GJs, due to the obstruction of the clouds and the heavy light pollution, only the FDJ and the trailing jet stages were clearly discernible on the video footage. Although the GJs were at a relatively large distance of ~210 km from the optical observation site, the accompanying in-cloud optical flashes at the GJ initiation are discernible. As a result, twelve out of the 14 GJs (>80%) were found to have the associated optical flashes from the GJ initiation. The other two no-flash GJs occurred back to back within a 1.5 min window. It may be that the clouds at this period were exceptionally thick and thus blocked the optical emissions from the initiating lightning to leak through. The ULF and the ELF/VLF signals are used to correlate the flashes in the optical fields. For example, the enhanced cloud illuminations in the field 1 of Figures 2a, 3a, and 4a are associated with the GJ initiating lightning, and they are within the yellow-shaded windows in Figures 2b, 3b, and 4b. Hence it is a strong indication that these optical flashes indeed come from the initiating lightning that preceded the leading jet [*Soula et al.*, 2011].

4.2. The Morphology and the Luminous Duration of Gigantic Jets

[14] The morphology of the 14 negative GJs can be grouped into the tree-like GJ (Figure 2a), the carrot-like GJ (Figure 3a), and the tree-carrot-like GJ (Figure 4a). In the FDJ stage of the tree-like GJs, the bright streamers propagate all the way from cloud top to the lower edge of the ionosphere, and featuring a fanning tree-like upper luminous body. However, the brightness of the streamers in the luminous upper body becomes wider and fainter as the altitude increases. For the carrot-like GJs, the bright streamers in the upper luminous body of the FDJ stops at an altitude of ~70 km, a dim gap exists between 70 and 80 km, and then a diffuse crown appears near the lower ionosphere boundary (80 ~ 90 km). A few carrot-like GJs have luminous beads structures in the lower streamer regions and the middle dim gap. For the hybrid tree-carrot-like GJs, the morphology of the FDJs in these events first appears to be a carrot-like, having a lower body of bright streamers, a dim middle gap with beads, and an upper diffusive crowning glow. However, in the subsequent frames, the streamers appear to increase in numbers and the beads also seem to brighten to fill the gap, and the FDJ transforms into a tree-like form. Finally, they fade away. Hence this is the reason why this group of events is termed as the "tree-carrot-like" GJs. Following the FDJ stage of different forms of GJs, a long lasting trailing jet

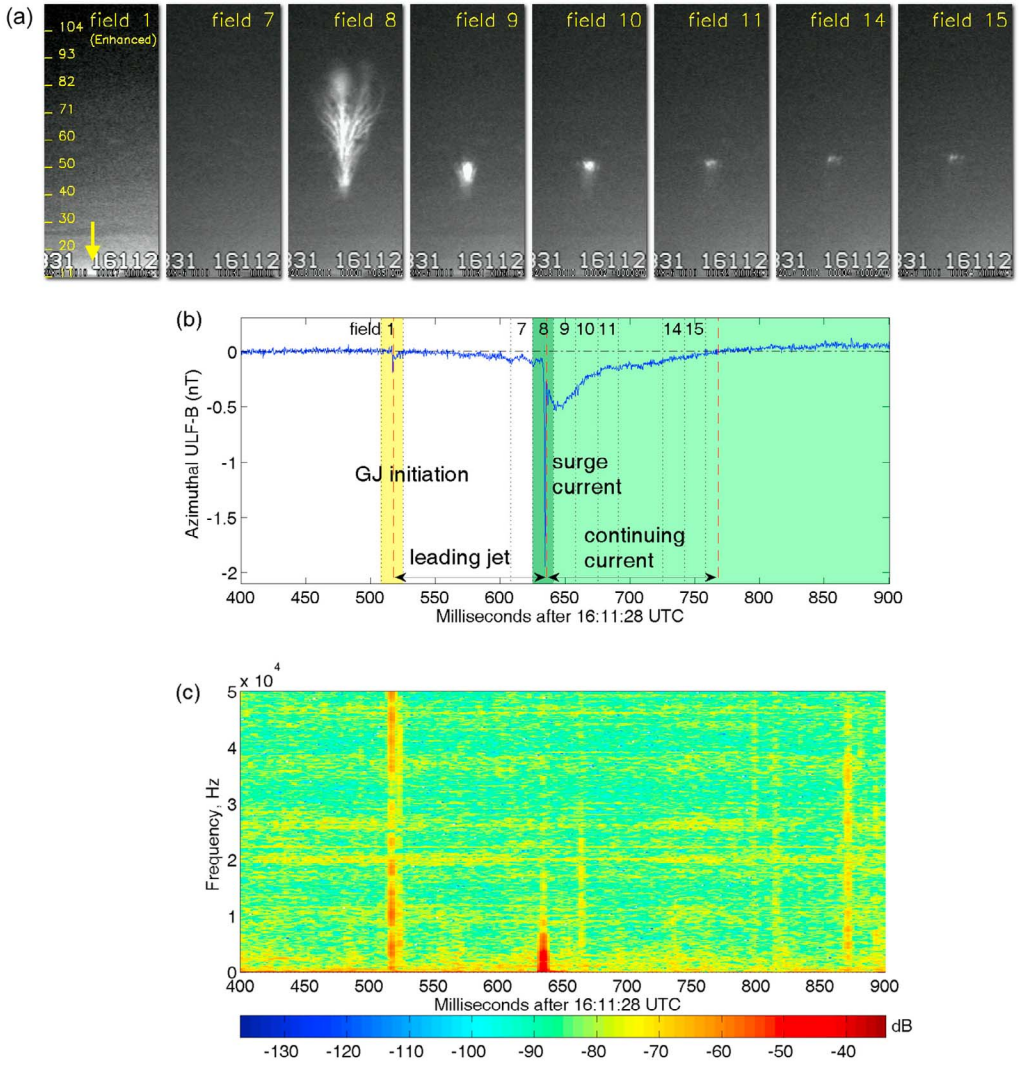

Figure 2. Selected R camera image fields, ULF sferics, and the ELF/VLF spectrogram of the tree-like GJ at 16:11:28 UTC on 31 August 2010. (a) Selected image fields showing the GJ initiation (field 1, enhanced), the fully developed jet (field 8), and the trailing jet (fields 9–15). (b) ULF sferics showing notable features associated with the GJ initiation (yellow), a negative fast descending pulse at the time of the connection between GJ and the ionosphere from the fully developed jet (dark green), and a long negative excursion pulse associated with the continuing current from the trailing jet (light green). (c) Spectrogram of ELF/VLF electric fields associated with the GJ.

was seen to rise up from the lower edge of the FDJs. From the optical images, the tree-like GJs seem to have the brightest trailing jets, the trailing jets for the tree-carrot-like GJs are slightly dimmer, and the trailing jets for the carrot-like GJs appears to be the dimmest.

[15] The three different morphologies of negative GJs also exhibit considerable difference in the luminous duration of the FDJ stage and the combined luminous duration of FDJ and trailing jet stages. As shown in Table 1, the carrot-like GJs have the longest FDJ duration (7 ∼ 9 fields; 100 ∼ 150 ms), while the tree-like GJs have the shortest (1 ∼ 4 fields; less than 67 ms). The carrot-like GJ also has the longest combined luminous durations (29 ∼ 45 fields; 467 ∼ 750 ms), and most of the tree-like and the tree-carrot-like GJs have shorter durations (16 ∼ 36 fields; 250 ∼ 600 ms and 15 ∼ 32 fields; 233 ∼ 530 ms, respectively).

5. The ULF and ELF/VLF Features of the Negative Gigantic Jets

[16] In this section, the association between the optical band data and the ULF and ELF/VLF radio signals is explored, especially on the signatures of the initiating lightning, the leading jet, the fully developed jet (FDJ), and the trailing jet for each group of negative GJs.

[17] Before the GJ initiation, it has been known that there is a preceding intracloud lightning development to amplify the charge imbalance in the cloud, and such intracloud

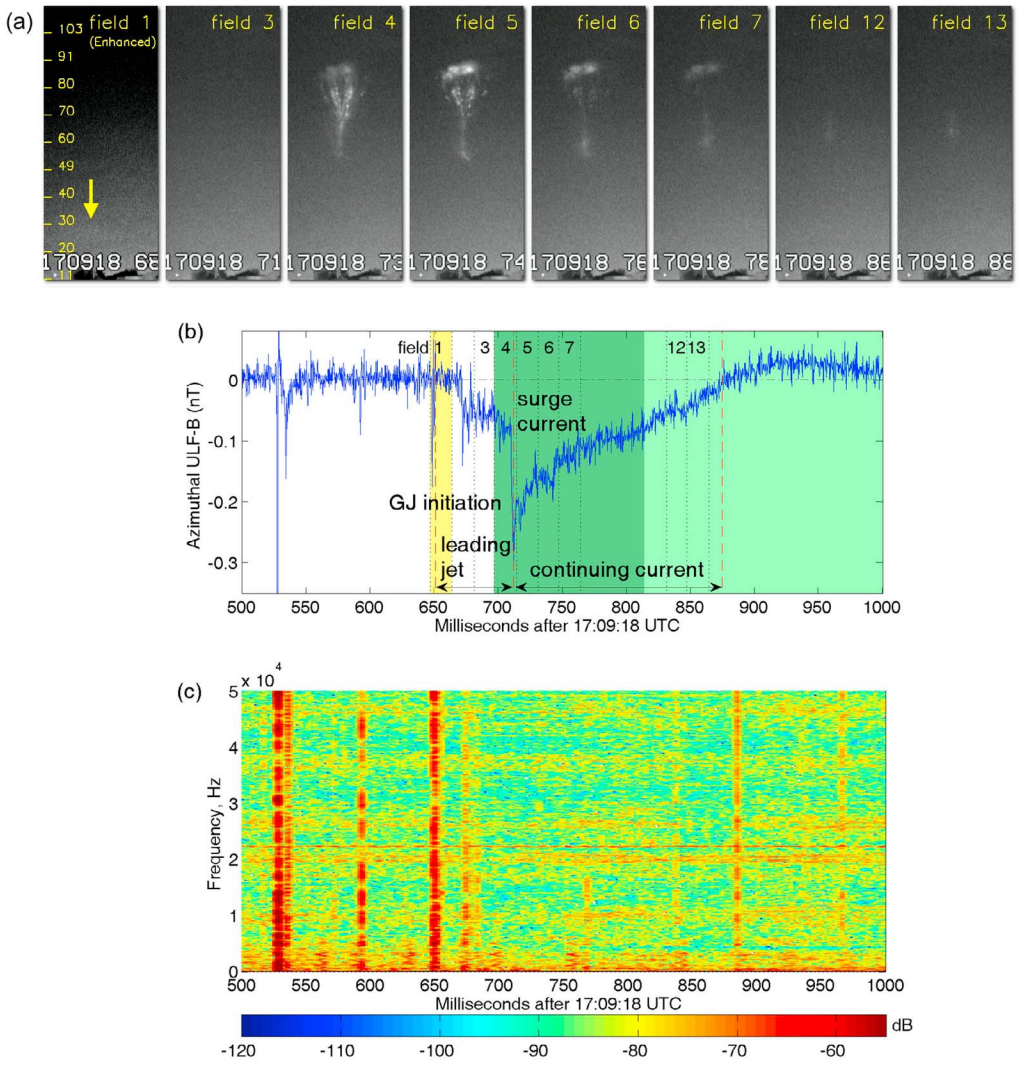

Figure 3. Selected R camera image fields, ULF sferics, and the ELF/VLF spectrogram of the carrot-like GJ at 17:09:18 UTC on 31 August 2010. (a) Selected image fields showing the GJ initiation (field 1, enhanced), the fully developed jet (field 4), and the trailing jet (fields 12 and 13). (b) ULF sferics showing notable features associated with the GJ initiation (yellow), a negative fast descending pulse at the time of the connection between GJ and the ionosphere from the fully developed jet (dark green), and a long negative excursion pulse associated with the continuing current from the trailing jet (light green). (c) Spectrogram of ELF/VLF electric fields associated with the GJ.

activity can begin with an narrow bipolar event (NBE), which typically has a time scale of ~10–20 μs [*Lu et al.*, 2011]. However, due to the low upper cutoff frequency of the NCKU ULF and ELF/VLF stations, no signature of the NBE can be discerned in the recorded signals.

5.1. Radio Signals Associated With the Initiating Lightning (the Gigantic Jet Initiation)

[18] As it has been stated in section 4.1, >80% of events had identifiable initiating lightning flashes in the images of GJs. However, all the GJs were found to have corresponding impulse signals, which were terms as the gigantic jet initiation [*Lu et al.*, 2011], in the ULF and ELF/VLF band data. Thus, it is a strong indication that the discharge at the initiation of GJs indeed is an integral process of the GJ discharges. Moreover, the spectrograms of the ELF/VLF signals in Figures 2c, 3c, and 4c show that the initiating signals have the signatures of a fast and broadbanded discharge, which are similar to those for the lightning discharge. Although the current ELF/VLF data are unable to differentiate whether the cloud illumination was due to intracloud (IC) or cloud-to-ground (CG) lightning, these data support that a negative GJ begins with initiating lightning that also produces the observable in-cloud illumination [*Lu et al.*, 2011]. The peak current moment (CM) and the charge moment change (CMC) of the initiating lightning for each type of GJs are inferred and summarized in Figure 5. It is interesting to note that different groups of GJs seem to

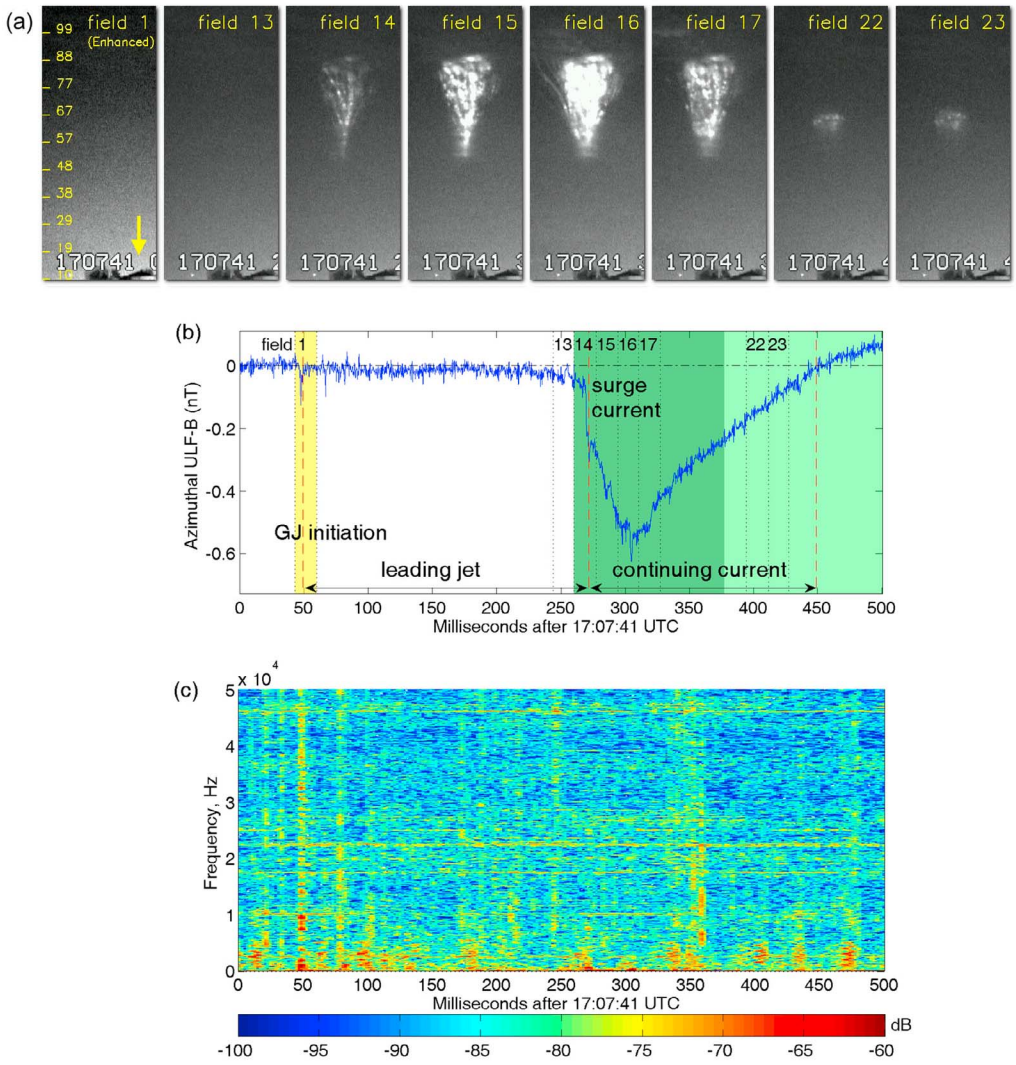

Figure 4. Selected R camera image fields, ULF sferics, and the ELF/VLF spectrogram of the hybrid tree-carrot-like GJ at 17:07:41 UTC on 31 August 2010. (a) Selected image fields showing the GJ initiation (field 1, enhanced), the fully developed jet (field 14), and the trailing jet (fields 22 and 23). (b) ULF sferics showing notable features associated with the GJ initiation (yellow), a negative fast descending pulse at the time of the connection between GJ and the ionosphere from the fully developed jet (dark green), and a long negative excursion pulse associated with the continuing current from the trailing jet (light green). (c) Spectrogram of ELF/VLF electric fields associated with the GJ.

exhibit different trends; indicating that the morphology of negative GJs may have been constrained by the GJ initiation.

5.2. Radio Signals Associated With the Leading Jet

[19] Due to the obstruction of the near clouds and the light-polluted sky over the NCKU site at the inner city, no leading jet of the 14 GJs was discernible in the optical image footage. However, every GJ has an ULF signal associated with the leading jet. The corresponding ULF signal contains a slow ramping feature, which is believed to be emitted by the upward moving negative leaders that follow the GJ initiation [*Cummer et al.*, 2009; *Lu et al.*, 2011]. As it was inferred from the ULF signal, the duration of the leading jet ranges from 24 ms to 225 ms with a medium value of 57 ms. Meanwhile, the CMC was found to fall between 39 and 678 C-km with a medium of 354 C-km. This new data set further confirms the slow ULF ramp is a generic feature of the leading jet stage in different forms of negative GJs.

5.3. Radio Signals Associated With the Fully Developed Jet (the GJ-Ionosphere Connection, the Surge Current)

[20] When the leading jet reaches the ionosphere, the GJ evolves into the FDJ stage. At the moment of the GJ-ionosphere contact, the ULF waveforms for various forms of negative GJs contain a fast descending signal from the surge current that flows in the discharge channel. The ULF waveform of the tree-like GJ (Figure 2b) shows a canyon-shaped drop at the beginning of FDJ (Figure 2a, field 8). For the carrot-like and the tree-carrot-like GJs, their ULF waveforms have the

Table 1. The Duration of the FDJ, the Combined Duration of FDJ and Trailing Jet, the Current Moment (CM), and the Charge Moment Change (CMC) of the Surge Current and the Continuing Current for the Three Forms of Negative Gigantic Jets[a]

Form of Gigantic Jet	Number of Events	Optical FDJ		Optical FDJ and Trailing Jet		Sferics Surge Current and Continuing Current			
		Duration in Number of Image Fields	Duration in Estimated ms	Duration in Number of Image Fields	Duration in Estimated ms	Surge CM in kA-km	Peak CM of Continuing Current in kA-km	CMC in C-km	Total Duration in ms
Tree-like	6	**1 ~ 4 (1)**	**0 ~ 67 (8)**	16 ~ 36 (23)	250 ~ 600 (375)	**60 ~ 159 (106)**	27 ~ 79 (51)	2720 ~ 4957 (3571)	137 ~ 283 (229)
Tree-carrot-like	5	**5 ~ 7 (6)**	**67 ~ 117 (92)**	15 ~ 32 (20)	233 ~ 533 (325)	18 ~ 36 (29)	**39 ~ 71 (54)**	**3166 ~ 5573 (4624)**	171 ~ 291 (203)
Carrot-like	3	**7 ~ 9 (8)**	**100 ~ 150 (125)**	**29 ~ 45 (42)**	**467 ~ 750 (692)**	16 ~ 22 (19)	**25 ~ 27 (26)**	**1790 ~ 3118 (2743)**	167 ~ 309 (245)

[a]Median is given in parentheses. The boldface types emphasize the typical values in the three forms of negative GJs.

cliff-shaped drops at the beginning of FDJ (Figure 3a, field 4 and Figure 4a, field 14). From the recorded ULF signals, the surge current moments (CM) at the GJ-ionosphere contact are derived and the results are listed in Table 1. Obviously, the tree-like GJs have the largest surge CMs, which are all greater than 60 kA-km and even up to 159 kA-km. The intense and impulse natures of the charge transfer at the GJ-ionosphere contact render the forms of the associated ULF signal waveforms being similar to those emitted during the CG return strokes. In contrast, the surge CM and the current for the tree-carrot-like and the carrot-like GJs are relatively small, less than 36 kA-km and 0.5 kA, respectively. Also, from the spectrogram of the associated ELF/VLF signals of the GJ-ionosphere contact, the frequency of the major radio emissions of the surge current is lower than 15 kHz, which is in sharp contrast to the impulsive nature of the initiating lightning while is similar to the sprite current, which has negligible VLF energy [*Cummer et al.*, 1998, 2006].

5.4. Radio Signals Associated With the Trailing jet (the Continuing Current)

[21] Figures 2b, 3b, and 4b show that in the ULF data, long continuing current waveform follows the FDJ-associated surge current for the GJs. As shown in Table 1, the peak CM of the continuing current for both the tree-like and the tree-carrot-like GJs has a large peak current moment (>27 kA-km and >39 kA-km, respectively) as inferred from the ULF sferics, while that for the carrot-like GJs is relatively small (<27 kA-km). The combined CMCs of the surge current and the continuing current in the FDJ and trailing jet stages are also listed in Table 1 and both show the same trend. The tree-carrot-like GJs have a larger combined charge moment change (>3166 C-km) comparing to that of the carrot-like GJs (<3118 C-km).

[22] Due to the slow varying nature of the continuing current flowing at this stage, it is believed that the distinct signals embedded in the spectrograms, Figures 2c, 3c, and 4c, are coincidental signals from nonrelated discharge processes and the currents associated with the trailing jets radiated no ELF/VLF band emissions. The spectrograms for the ULF band signals are also examined (not shown) and the

Figure 5. The peak current moment (CM) versus the charge moment change (CMC) diagram for the initiating lightning of the 14 negative GJs. The markers are blue squares for the tree-like GJs, red circles for the tree-carrot-like GJs, and black crosses for the carrot-like GJs.

major frequencies of their emissions are found to stay below 20 Hz.

6. Discussion: GJ Morphologies and the Underlying Discharge Parameters

[23] The cloud top emerging height for these negative GJs is ∼15 km [*Su et al.*, 2003; *Chou et al.*, 2011]. Since the termination height of these GJs is at ∼90 km (see section 3), the discharge channel length for the FDJs is ∼75 km. Thus with the current moment (CM) being 60 ∼ 159 kA-km, the surge current for the tree-like GJs are computed to be 0.8 ∼ 2.1 kA, which is generally larger than the 0.73 kA reported in *Cummer et al.* [2009]. However, if the estimated channel length shortens or lengthens by 5 km (∼7%), the inferred surge current would vary by ∼10%.

[24] As depicted in Figure 2a, the luminous duration of the FDJ for tree-like GJs is brief and lasts no more than one to four image fields (less than 67 ms; Table 1). It may be that for this form of negative GJs the surge CM at the GJ-ionosphere contact is large enough to cause a sufficiently high degree of ionization at the upper trunk of GJs. Therefore, the upper discharge channel is practically shorted-out and causes the local ionosphere boundary drops down to ∼50 km [*Kuo et al.*, 2009] in less than one image field (less than 17 ms). Hence the discharge channel for the trailing continuing current is ∼35 km in length. With this channel length, the continuing currents are inferred to range between 0.77 kA and 2.26 kA; the large currents are consistent with the bright trailing jets seen in the optical band data (Figure 2a).

[25] The surge CMs of carrot-like and tree-carrot-like GJs are 16 kA-km to 36 kA-km, which are substantially lower than those for tree-like GJs. With the same assumed channel length (∼75 km), the corresponding surge currents at the GJ-ionosphere contact range between 0.16 kA and 0.48 kA for these two forms of GJs. The small surge CMs could explain why the FDJs for these two categories of GJs are relatively dim and mingling with nonluminous gaps as well as diffusive crowns as they first formed (Figures 3a and 4a). Besides, their further developments are remarkably different. As for the carrot-like GJs, the trailing continuing CMs are the smallest (0.33 kA to 0.36 kA) among the trio, and this may explain why the dim upper trunks of the FDJs soon fade away and the trailing jets are also dim. The tree-carrot-like GJs have a larger continuing CMs (39 kA-km to 71 kA-km) comparing to those for the carrot-like GJs, thus it may imply that, during the transformation from carrot-like to tree-like GJs, a higher number of streamers have been generated, causing the upper trunk to brighten up and eventually produce clearly discernible trailing jets. Also in contrast to the tree-like GJs, the local ionosphere boundary height for the carrot-like and the tree-carrot-like GJs remains unaffected for a notably longer period (5 ∼ 9 image fields; 67 ∼ 150 ms). It is possible that, for smaller surge currents, longer time is needed to build up enough ionization at the upper trunk and cause the local ionosphere boundary to drop.

[26] The aforementioned results seem to imply that the magnitude of the surge current is a crucial factor in determining the form of the negative GJs. If a negative GJ starts with a sufficiently large surge CM, >60 kA-km, for the events analyzed in this work, a tree-like GJ is formed; at the same time the ionization at the upper trunk is sufficiently high to short-out the discharge channel and to lower the local ionosphere boundary. Whereas, if the surge CM is relatively small, <36 kA-km, carrot-like or tree-carrot-like GJs are formed and the local ionosphere boundary remains unaffected for an extended period. The deciding factor separating the latter two forms of GJs appears related to the magnitude of the trailing continuing current. If the follow-up continuing CMs are relatively large, >39 kA-km as inferred from the data, the current will enhance the luminosity of the upper trunk of the FDJs and supplies a bright trailing jet in the case of the tree-carrot-like GJs. If the trailing continuing CMs are less than 27 kA-km, dim carrot-like GJs with very dim trailing jets are formed.

[27] For the carrot-like and tree-carrot-like GJs, their morphology, the lower streamer region, the middle nonluminous gap and the upper diffuse top are very similar to those in a sprite. *Pasko et al.* [1998] and *Pasko and Stenbaek-Nielsen* [2002] proposed that the diffuse, transition and streamer regions in sprites result from the interplay of the dissociative attachment time scale, the ambient dielectric relaxation time scale, and the time scale for the development of an individual electron avalanche into a streamer. We believe that these time scales may have also played similar roles in affecting the spatial structures of the negative gigantic jets reported here.

7. Conclusion

[28] Dozens of gigantic jets were observed to occur over Typhoon Lionrock (2010) in a 6 hour interval on the night of 31 August 2010. The occurring locations of the GJs were inferred to be over a convective cell that located at the eyewall. It is believed that, in this eyewall convective core, the charge structure has been dislocated by the vertical wind shear and thus causes GJs to occur more easily over the protruding cloud top. Therefore, with these attributes, Typhoon Lionrock (2010) has become a prolific system in the production of gigantic jets. Among the 14 negative GJs analyzed in this work, besides the previously recognized tree-like and carrot-like GJs, a third intermediate type called tree-carrot-like form was identified. The complementary ULF and ELF/VLF band data for these GJs contain signals from the GJ initiation, the leading jet, the surge current, and the continuing current, which are respectively associated with the initiating lightning, the leading jet, the fully developed jet (FDJ), and the trailing jet stages of the optical band data. For the GJ events analyzed in this work, >80% of them are found to have recognizable optical emissions from the initiating lightning. The absence of signals from initiating lightning for the other events is likely due to the obstruction of clouds and light pollution at the inner city observation site, since all the events were detected with signals from this process in the ELF/VLF data. Nevertheless, our observations are consistent with that the initiating intracloud lightning process is an integral process of negative GJ evolution.

[29] The three forms of negative GJs are distinct in their morphology and in the luminous duration of the FDJ and trailing jet stages. The peak current moments (CMs) of the surge currents, the peak CM of the continuing currents and the charge moment change (CMC) of the surge and the continuing currents are important parameters in determining the forms of the negative GJs. When the peak CM of the

surge currents exceeds 60 kA-km, tree-like GJs are produced with a bright but brief FDJ stage. While if the surge CM is less than 36 kA-km, carrot-like and tree-carrot-like GJs are produced. The peak CM of the continuing current following the FDJs appears to be the next factor separating the carrot-like and tree-carrot-like GJs. If the peak CM is less than 25 kA-km, dim carrot-like GJs with very dim trailing jets are formed. The available data indicate that, if the peaks CMs are 39 $\sim$ 71 kA-km, tree-carrot-like GJs are formed and the trailing jets are also relatively bright. Finally, the peak current moment (CM) versus charge moment change (CMC) diagram for the initiating lightning seems to imply that different groups of GJs have different occurrence trends. This feature suggests that the forms of negative GJs may have been determined at the initiating stage.

[30] **Acknowledgments.** We thank Steve A. Cummer for fruitful discussions on various aspects of ULF/ELF/VLF recording and data processing systems. We wish to thank the World Wide Lightning Location Network (http://wwlln.net) for providing the lightning location data used in this paper. We are grateful to the Lulin Observatory, National Central University, and the Cingcao elementary school for hosting our ULF and ELF/VLF stations. This work was supported in part by grants NSPO-S-100010, NSC 100-2111-M-006-002, NSC 99-2112-M-006-006-MY3, NSC 99-2111-M-006-001-MY3, NSC 100-2111-M-006-001, NSC 100-2119-M-006-014, and NSC 100-2119-M-006-015.

[31] Robert Lysak thanks the reviewers for their assistance in evaluating this paper.

References

Bilitza, D., and B. W. Reinisch (2008), International Reference Ionosphere 2007: Improvements and new parameters, *Adv. Space Res.*, *42*, 599–609, doi:10.1016/j.asr.2007.07.048.

Boeck, W. L., O. H. Vaughan Jr., R. J. Blakeslee, B. Vonnegut, M. Brook, and J. McKune (1995), Observations of lightning in the stratosphere, *J. Geophys. Res.*, *100*(D1), 1465–1475, doi:10.1029/94JD02432.

Chen, A. B., et al. (2008), Global distributions and occurrence rates of transient luminous events, *J. Geophys. Res.*, *113*, A08306, doi:10.1029/2008JA013101.

Chern, J. L., R. R. Hsu, H. T. Su, S. B. Mende, H. Fukunishi, Y. Takahashi, and L. C. Lee (2003), Global survey of upper atmospheric transient luminous events on the ROCSAT-2 satellite, *J. Atmos. Sol. Terr. Phys.*, *65*, 647–659, doi:10.1016/S1364-6826(02)00317-6.

Chou, J. K., et al. (2010), Gigantic jets with negative and positive polarity streamers, *J. Geophys. Res.*, *115*, A00E45, doi:10.1029/2009JA014831.

Chou, J. K., L. Y. Tsai, C. L. Kuo, Y. J. Lee, C. M. Chen, A. B. Chen, H. T. Su, R. R. Hsu, P. L. Chang, and L. C. Lee (2011), Optical emissions and behaviors of the blue starters, blue jets, and gigantic jets observed in the Taiwan transient luminous event ground campaign, *J. Geophys. Res.*, *116*, A07301, doi:10.1029/2010JA016162.

Cummer, S. A., U. S. Inan, T. F. Bell, and C. P. Barrington-Leigh (1998), ELF radiation produced by electrical currents in sprites, *Geophys. Res. Lett.*, *25*, 1281–1284, doi:10.1029/98GL50937.

Cummer, S. A., H. U. Frey, S. B. Mende, R.-R. Hsu, H.-T. Su, A. B. Chen, H. Fukunishi, and Y. Takahashi (2006), Simultaneous radio and satellite optical measurements of high-altitude sprite current and lightning continuing current, *J. Geophys. Res.*, *111*, A10315, doi:10.1029/2006JA011809.

Cummer, S. A., J. Li, F. Han, G. Lu, N. Jaugey, W. A. Lyons, and T. E. Nelson (2009), Quantification of the troposphere-to-ionosphere charge transfer in a gigantic jet, *Nat. Geosci.*, *2*, 617–620, doi:10.1038/ngeo607.

Dowden, R. L., J. B. Brundell, and C. J. Rodger (2002), VLF lightning location by time of group arrival (TOGA) at multiple sites, *J. Atmos. Sol. Terr. Phys.*, *64*, 817–830, doi:10.1016/S1364-6826(02)00085-8.

Hsu, R. R., H. T. Su, A. B. Chen, L. C. Lee, M. Asfur, C. Price, and Y. Yair (2003), Transient luminous events in the vicinity of Taiwan, *J. Atmos. Sol. Terr. Phys.*, *65*, 561–566, doi:10.1016/S1364-6826(02)00320-6.

Huang, S.-M., C.-L. Hsu, A. B. Chen, J. Li, L.-J. Lee, G.-L. Yang, Y.-C. Wang, R.-R. Hsu, and H.-T. Su (2011), Effects of notch-filtering on the ELF sferics and the physical parameters, *Radio Sci.*, *46*, RS5014, doi:10.1029/2010RS004519.

Krehbiel, P. R., J. A. Riousset, V. P. Pasko, R. J. Thomas, W. Rison, M. A. Stanley, and H. E. Edens (2008), Upward electrical discharges from thunderstorms, *Nat. Geosci.*, *1*, 233–237, doi:10.1038/ngeo162.

Kuo, C.-L., et al. (2009), Discharge processes, electric field, and electron energy in ISUAL-recorded gigantic jets, *J. Geophys. Res.*, *114*, A04314, doi:10.1029/2008JA013791.

Lee, L.-J., S.-M. Huang, J.-K. Chou, C.-L. Kuo, A. B. Chen, H.-T. Su, R.-R. Hsu, H. U. Frey, Y. Takahashi, and L.-C. Lee (2012), Characteristics and generation of secondary jets and secondary gigantic jets, *J. Geophys. Res.*, *117*, A06317, doi:10.1029/2011JA017443.

Lu, G., et al. (2011), Lightning development associated with two negative gigantic jets, *Geophys. Res. Lett.*, *38*, L12801, doi:10.1029/2011GL047662.

Lyons, W. A., T. E. Nelson, R. A. Armstrong, V. P. Pasko, and M. A. Stanley (2003), Upward electrical discharges from thunderstorm tops, *Bull. Am. Meteorol. Soc.*, *84*(4), 445–454, doi:10.1175/BAMS-84-4-445.

Marshall, R. A., and U. S. Inan (2007), Possible direct cloud-to-ionosphere current evidenced by sprite-initiated secondary TLEs, *Geophys. Res. Lett.*, *34*, L05806, doi:10.1029/2006GL028511.

Pasko, V. P. (2008), Blue jets and gigantic jets: Transient luminous events between thunderstorm tops and the lower ionosphere, *Plasma Phys. Controlled Fusion*, *50*(12), 124050, doi:10.1088/0741-3335/50/12/124050.

Pasko, V. P. (2010), Recent advances in theory of transient luminous events, *J. Geophys. Res.*, *115*, A00E35, doi:10.1029/2009JA014860.

Pasko, V. P., and H. C. Stenbaek-Nielsen (2002), Diffuse and streamer regions of sprites, *Geophys. Res. Lett.*, *29*(10), 1440, doi:10.1029/2001GL014241.

Pasko, V. P., U. S. Inan, and T. F. Bell (1998), Spatial structure of sprites, *Geophys. Res. Lett.*, *25*, 2123–2126, doi:10.1029/98GL01242.

Pasko, V. P., M. A. Stanley, J. D. Mathews, U. S. Inan, and T. G. Wood (2002), Electrical discharge from a thundercloud top to the lower ionosphere, *Nature*, *416*, 152–154, doi:10.1038/416152a.

Pasko, V. P., Y. Yair, and C.-L. Kuo (2012), Lightning related transient luminous events at high altitude in the Earth's atmosphere: Phenomenology, mechanisms and effects, *Space Sci. Rev.*, *168*, 475–516.

Riousset, J. A., V. P. Pasko, P. R. Krehbiel, W. Rison, and M. A. Stanley (2010), Modeling of thundercloud screening charges: Implications for blue and gigantic jets, *J. Geophys. Res.*, *115*, A00E10, doi:10.1029/2009JA014286.

Rodger, C. J., S. Werner, J. B. Brundell, E. H. Lay, N. R. Thomson, R. H. Holzworth, and R. L. Dowden (2006), Detection efficiency of the VLF World-Wide Lightning Location Network (WWLLN): Initial case study, *Ann. Geophys.*, *24*, 3197–3214, doi:10.5194/angeo-24-3197-2006.

Soula, S., O. van der Velde, J. Montanya, P. Huet, C. Barthe, and J. Bór (2011), Gigantic jets produced by an isolated tropical thunderstorm near Réunion Island, *J. Geophys. Res.*, *116*, D19103, doi:10.1029/2010JD015581.

Su, H.-T., R.-R. Hsu, A. B.-C. Chen, Y.-J. Lee, and L.-C. Lee (2002), Observation of sprites over the Asian continent and over oceans around Taiwan, *Geophys. Res. Lett.*, *29*(4), 1044, doi:10.1029/2001GL013737.

Su, H. T., R. R. Hsu, A. B. Chen, Y. C. Wang, W. S. Hsiao, W. C. Lai, L. C. Lee, M. Sato, and H. Fukunishi (2003), Gigantic jets between a thundercloud and the ionosphere, *Nature*, *423*, 974–976, doi:10.1038/nature01759.

van der Velde, O. A., W. A. Lyons, T. E. Nelson, S. A. Cummer, J. Li, and J. Bunnell (2007), Analysis of the first gigantic jet recorded over continental North America, *J. Geophys. Res.*, *112*, D20104, doi:10.1029/2007JD008575.

van der Velde, O. A., J. Bór, J. Li, S. A. Cummer, E. Arnone, F. Zanotti, M. Füllekrug, C. Haldoupis, S. NaitAmor, and T. Farges (2010), Multi-instrumental observations of a positive gigantic jet produced by a winter thunderstorm in Europe, *J. Geophys. Res.*, *115*, D24301, doi:10.1029/2010JD014442.

Wang, Y.-C., K. Wang, H.-T. Su, and R.-R. Hsu (2005), Low-latitude ELF-whistlers observed in Taiwan, *Geophys. Res. Lett.*, *32*, L08102, doi:10.1029/2005GL022412.

Wescott, E. M., D. Sentman, D. Osborne, D. Hampton, and M. Heavner (1995), Preliminary results from the Sprites94 Aircraft Campaign: 2. Blue jets, *Geophys. Res. Lett.*, *22*(10), 1209–1212, doi:10.1029/95GL00582.

Wescott, E. M., D. D. Sentman, M. J. Heavner, D. L. Hampton, D. L. Osborne, and O. H. Vaughan Jr. (1996), Blue starters: Brief upward discharges from an intense Arkansas thunderstorm, *Geophys. Res. Lett.*, *23*(16), 2153–2156, doi:10.1029/96GL01969.

Wu, C.-C., T.-S. Huang, W.-P. Huang, and K.-H. Chou (2003), A new look at the binary interaction: Potential vorticity diagnosis of the unusual southward movement of Tropical Storm Bopha (2000) and its interaction with Supertyphoon Saomai (2000), *Mon. Weather Rev.*, *131*, 1289–1300, doi:10.1175/1520-0493(2003)131<1289:ANLATB>2.0.CO;2.